Chiang Mai J. Sci. 2016; 43(2) : 320-328
http://epg.science.cmu.ac.th/ejournal/
Contributed Paper

Preparation of Nano-hydroxyapatite Particles by Ultrasonic Method at 25 kHz Using Natural Rubber Latex as a Templating Agent

Songkot Utara [a,b]*, Jutharatana Klinkaewnarong [a,c]
[a] Polymer and Material Research Groups.
[b] Division of Chemistry, Faculty of Science, Udon Thani Rajabhat University, Udon Thani 41000, Thailand.
[c] Program in Physics, Faculty of Science, Udon Thani Rajabhat University, Udon Thani 41000, Thailand.
*Author for correspondence; e-mail: songkot_u@hotmail.com; songkot@udru.ac.th.

Received: 15 September 2015
Accepted: 2 November 2015

ABSTRACT

Natural rubber latex (1% DRC) was used as a templating agent for the preparation of nano-hydroxyapatite (HAp) powder using an *ultrasonic* technique at a constant temperature of 25°C (25 kHz). Di-ammonium hydrogen phosphate ($(NH_4)_2$ HPO_4) and calcium nitrate tetrahydrate ($Ca(NO_3)_2.4H_2O$) were used as starting materials. The study investigated the effects of increasing sonication time (0, 20, 40 and 60 min) and effect of Ca:P ratios (1.67 and 1.50) on the properties of calcium phosphate ($Ca_{10-x}(HPO_4)_x(PO_4)_{6-x}(OH)_{2-x}$, $x = 0$ and $x = 1$). To obtain HAp, latex containing calcium phosphate was dried at 60°C and calcined at 600°C for 2 hours. The thermal properties, crystallinity, functionality and morphology of the powders were evaluated using thermo-gravimetric analysis (TGA), X-ray diffraction (XRD), Fourier transform Raman spectroscopy (FT-Raman) and transmission electron microscopy (TEM). The XRD results confirmed formation of mixed phases of HAp and β-TCP in all synthesised HAp samples. Both the crystalline size and crystalline material fraction (as %) of $x = 0$ were higher than for $x = 1$. After 20 minutes, these two properties tended to decrease with increasing sonication time. FT-Raman studies also revealed the presence of OH^- in the hydroxyapatite phase with longer sonication times, with the ($\nu_1(PO^{-3}_4)$) mode (962 cm^{-1}) being present for both $x = 0$ and $x = 1$. TEM images demonstrated decreasing HAp particle diameters with increasing sonication time. These subsequently formed longer, nano- rod-like shapes in the case of calcium-deficient HAp ($x = 1$).

Keywords: hydroxyapatite, ultrasonic method, natural rubber latex, templating agent

1. INTRODUCTION

Calcium phosphate is a known biomedical material found in hard tissue of the human body such as bone and teeth (enamel). Calcium phosphate is chemically similar to the inorganic component of bone matrix, hydroxyapatite ($Ca_{10}(OH)_2(PO_4)_6$, HAp)[1,2]. Additionally, HAp exhibits desirable properties such as good

biocompatibility, excellent ability to form chemical bonds with living bone tissue, and suitable osteoconductivity [1-3]. However, the effectiveness of HAp depends on its size. Nanostructural HAp with a high surface area is more desirable for use in many applications [4], e.g., fillers for improving the properties of dental adhesives [5], and drug and gene delivery agents [6]. Therefore, many attempts have been proposed for preparation of nano HAp. Shanthi *et al.* [7] reported a successful method to synthesize a porous shell-like nano hydroxyapatite using various surfactants and polymers as templates. They also suggested that templating macromolecules act as nucleation centers and morphology-determining agents as well as creating porosity after their removal.

Natural rubber latex (*Hevea brasiliensis*) is bio-macromolecule, which consists of *cis*-polyisoprene (hydrocarbon) and non-rubber components such as lipids, proteins and carbohydrate, among others [8-9]. Additionally, some trace elements occur in natural rubber latex such as Ca, K, Al, Na, Mg, Mn, Fe, Si, Rb, P, N, S and O [10]. Stabilization of rubber particles is due to the repulsion of negative charges, which are found on the surface of rubber particles. Nawamawat *et al.* [9] proposed that the surface of rubber particles is a mixed layer of proteins and phospholipids *ca.* 20 nm thick. Therefore, cations can be adsorbed on the surface of rubber particles [11-12]. Thus, addition of precursor cations for preparation of HAp, such as Ca^{2+}, can possibly be adsorbed on the surface rubber particles, resulting in a soft bio-macrocmolecular template.

Ultrasonic procedures are effective methods for synthesis of nanomaterials, nanocomposites, and nanoforms of chemical compounds. These processes are faster, have higher yields, and present the possibility of fabrication of novel compounds, substances or materials that are difficult or impossible to obtain via classic interactions [13]. HAp has been prepared using ultrasound [14-17]. Our previous work [17] showed that a longer ultrasonic irradiation for HAp resulted in a smaller particle size and a normal particle size distribution. Recently, the first time, a combination of ultrasonic (20kHz) and bio-macromolecular template methods (natural rubber latex) used for synthesis of nano-HAp was reported [18]. We found that smaller diameter, *ca* 8 nm, nano rod-like HAp particles were obtained with a 20 minute dose of ultrasonic irradiation in the case of non-stoichiometric HAp. Furthermore, natural rubber latex might act as a structure-directing agent in the formation of nano-strucrural HAp. In this paper, we demonstrated how ultrasonic irradiation at 25 kHz affected HAp crystal formation. Additionally, the effect of the Ca:P ratio and sonication time on the thermal properties, crystallinity, morphology and functional groups of HAp were also investigated.

2. MATERIALS AND METHODS

2.1 Materials

All starting materials used in this work were analytical grade: calcium nitrate ($Ca(NO_3)_2.4H_2O$) (99.9% purity, Kanto Chemical), di-ammonium hydrogen phosphate ($(NH_4)_2 HPO_4$) (99% purity, BDH), acetic acid (CH_3COOH) (100%, BDH Analar) and ammonium solution (28 wt.%, QRec, New Zealand). Deionised water was used for dilution of natural rubber latex. Freshly tapped latex was collected in a beaker from trees derived from the RRIM 600 clone and adjusted to pH 10 with dilute ammonium solution (0.6%v/v). Dry rubber content of latex was measured using standard methods (ISO126:2005). The number average molecular weight ($\overline{M}_n$) and weight average

molecular weight ($\overline{M}_w$) were measured using gel permeation chromatography [19]. The $\overline{M}_w$ and $\overline{M}_n$ were 2.94×10^5 g/mol and 2.41×10^6g/mol, respectively. The latex was then diluted with deionised water to obtain 1% DRC.

2.2 Sample Preparation

Synthesis of nano HAp particles was done using the same method as in our previous work [18]. Various Ca:P ratios (x = 0, 1) in 1% DRC natural rubber latex were used in the preparation of HAp nanoparticles of $Ca_{10-x}(PO_4)_{6-x}(HPO_4)_x(OH)_{2-x}$. The Ca:P ratios were fixed at 1.67 (x = 0) and 1.50 (x =1). In general, the Ca:P (1.67) is known as stoichiometric and the latter is also known as non-stoichiometric or calcium-deficiency apatite. In the case of x = 0, 2.5 M $Ca(NO_3)_2.4H_2O$ was prepared in 25 mL of latex using a magnetically stirred mixer at room temperature until it was homogeneous. Concurrently, 1.50 M of $(NH_4)_2HPO_4$ was also prepared in 25 mL of latex. After that, two solutions were mixed together in a 100 mL Schlenk flask (diameter = 5.0 cm). The Schlenk flask was placed in the ultrasonic reactor setup of our previous work [17-18]. The mixture was then continuously irradiated with ultrasonic waves (25 kHz) for 0, 20, 40, and 60 min. Throughout the sonication, the temperature of the reactor was monitored and controlled at 25±1 °C. After the desired time, the mixture was transferred into a 150 mL beaker and continuously mixed with a magnetic stirrer at 70 °C until dry. In order to determine the possible temperatures of decomposition and crystallization of the nano HAp, dried natural rubber was subjected to thermogravimetric differential thermal analysis (TG-DTA; Shimadzu's TGA-50). TG-DTA was run between 30° C and 1200 °C in dry air at a heating rate of 10 °C/min To obtain a HAp powder, the dried natural rubber was calcined in a Muffle furnace (M12/14P, Chavachote) at 600 °C at a heating rate of 3 °C/min. The phase purity and crystallinity of HAp powder were determined using an X-ray powder diffractometer (XRD, PW3710, The Netherlands) with Cu-Kα radiation (λ = 0.15406 nm). The line broadening of the (002), (211), (300), (202), (310), (222) and (213) reflections was used to evaluate the mean crystal size, L, of the prepared HAp powders, which was calculated from the equation [18,20]:

$$\beta_r\cos\theta = \frac{k\lambda}{L} + \eta\sin\theta$$

where λ is the X-ray wavelength , k is a constant (1), θ is diffraction angle, η is the observed deformation strain in the materials and β_r is the full width at half maximum (FWHM) and is given by $\beta_r^2 = \beta_o^2 - \beta_i^2$where β_o^2 and β_i are the width of the observed X-ray peak and the width due to instrumental effects, respectively. The crystalline phase fraction of HAp was determined using the equation below [18,21]:

$$X_c = \left(\frac{0.24}{\beta_{002}}\right)^3$$

where β_{002} is the FWHM of line broadening of the (002).The functional group of HAp powder was characterized using FT-Raman spectrometry (Bruker Vertex 70, RAM II). Additionally, the morphology of HAp was observed using transmission electron microscopy (TEM, TECNAI G2 20 S-TWIN). Image J analysis software was used to measure the diameter of HAp particles [17-18].

3. RESULTS AND DISCUSSION

In general, the thermal stability of HAp was strongly influenced by its Ca:P ratio. Thus, the decomposition temperature of

HAp qualitatively provided evidence about its Ca:P ratio [22]. Figure 1 (a) and (b) show the TGA-DTA curve of prepared HAp. From Figure 1(a), three decomposition steps were observed. The first step ranged from 25 to 270 °C. This step was the loss of adsorbed water in HAp powder [2, 18]. The second step was a major loss of mass (30%) between 270 and 550 °C. This step is due to thermooxidative properties of the natural rubber incorporated within the dehydrated nitrate and ammonium in the starting materials [18]. The last step ranged from 550 to 600 °C. It was found that almost no weight loss could be observed at above 600 °C, suggesting the formation of crystalline HAp. Therefore, in the case of $x = 0$, the prepared HAp was successfully obtained at 600 °C. From Figure 1(b), three decomposition steps were observed. Comparing $x = 0$ and $x = 1$, the last step of decomposition in the case of $x = 1$ began at around 480 °C, while in the case of $x = 0$, it began at about 550 °C. These findings suggest a lower crystallisation temperature for the non-stoichiometric case. In other words, a lower temperature for formation of crystalline HAp occured when $x = 1$. The results were supported by an observed lower thermal stability when $x = 0$ than when $x = 1$. It was found that the Ca:P ratio affected thermal stability of prepared HAp in the presence of natural rubber latex when used as a soft bio-macromolecule template. However, these results seem inconsistent with Viswanath and Ravishankar [22]. They found that non-stoichiometric material showed poor thermal stability in comparison to stoichiometric HAp. A possible explanation is that the natural rubber latex (template) plays an important role in the thermal stability of prepared HAp [18].

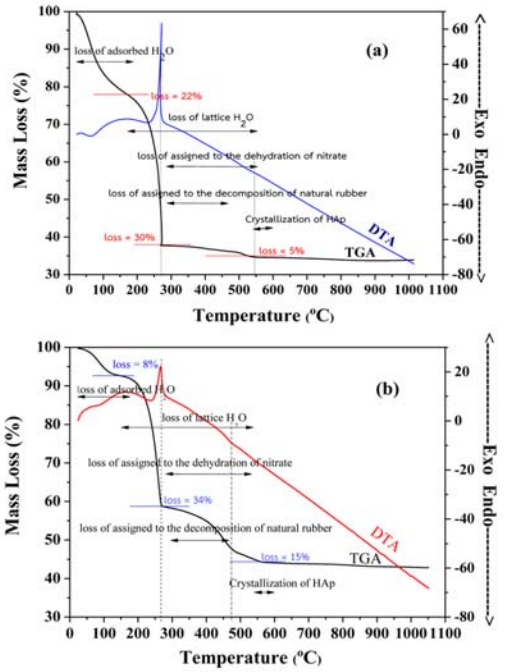

Figure 1. TGA-DTA curve of un-irradiated samples (a) $x = 0$ and (b) $x = 1$.

The effect of sonication time on the TGA curve of prepared HAp is shown in Figure 2. From this figure, it can be clearly seen that the decomposition step of stoichiometric HAp ($x = 0$) was unaltered by sonication time. Thus, it can be stated that the second decomposition step did not change significantly after sonication. More interestingly, in the case of non-stoichiometric HAp ($x = 1$), the second decomposition step shifted to lower temperatures with increasing sonication time (Figure 2(b)). These results reveal that the formation temperature of crystalline HAp transitioned to lower temperatures with increasing sonication time [18]. Thus, formation of non-stoichiometric HAp in the presence of natural rubber latex was altered by ultrasonic waves.

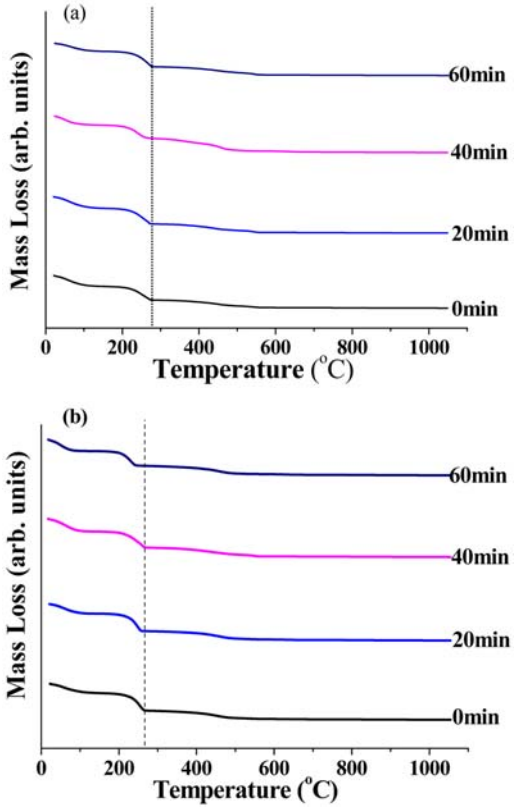

Figure 2. TGA curve of HAp (a) $x = 0$ and (b) $x = 1$.

The effect of sonication time on the XRD patterns is shown in Figure 3. The XRD patterns of the powders were typically of HAp, in agreement with published literature [1-7]. It was observed that all prepared HAp samples showed XRD peaks (002), (211), (300), (310) similar to those of standard data for HAp powder (JCPDS090432). From Figure 3(a), a small peak of β-tricalcium phosphate, β-TCP (JCPDS090169) was observed. Thus, in case of $x = 0$, a mixed phase of HAp and β-TCP was found in the absence of natural rubber latex. Interestingly, no phase change in HAp was observed when irradiated with ultrasonic waves [17,18]. From Figure 3 (b), XRD patterns also show the formation of HAp and β-TCP along with some calcium oxide (CaO) phase. This indicates that the decarbonation of HAp occured during preparation of HAp [23]. Comparing Figures 3 (a) and 3(b), the XRD patterns of $x = 0$ are significantly corresponding to $x = 1$ except for the peak width and absolute intensity. This significance shows the structure in non-stoichiometric HAp does not alter the basis crystalline arrangement. Additionally, the quantity of β-TCP in the case of $x = 1$ was higher than that when $x = 0$. The β-TCP phase showed better biocompatibility in comparison to the pure HAp phase [3].

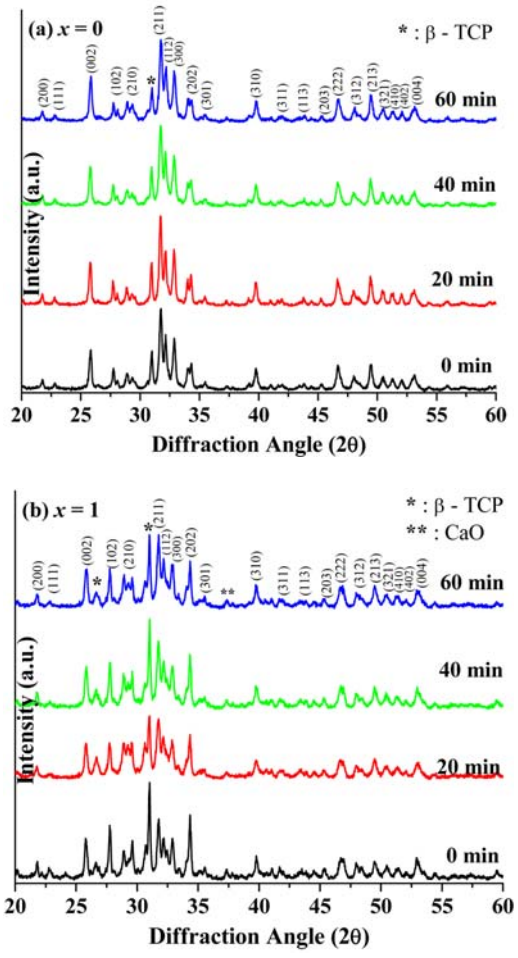

Figure 3. XRD patterns of HAp (a) $x = 0$ and (b) $x = 1$.

The mean crystal size and fraction of the crystalline phase of HAp are presented in Table 1. A large crystal size (53.01nm) was observed in case of $x = 0$ with a 20 minute dose of sonication. A smaller crystal size (22.32 mn) was observed in case of $x = 1$ at the same sonication time. Additionally, the fraction of crystalline phase of both $x = 0$ and $x = 1$ ranged from 0.54 to1.81. These results suggest that the crystal size as well as fraction of crystalline material is independent of sonication time [17-18].

Table 1. Mean crystal size from XRD line broadening calculated from XRD patterns and fraction of the crystalline phase of HAp.

Sonication time (min)	Crystal size (nm) from XRD line broadening		Fraction of the crystalline phase (X_c)	
	$x = 0$	$x = 1$	$x = 0$	$x = 1$
0	28.01	33.49	0.82	1.37
20	53.01	22.32	1.81	0.66
40	26.56	23.34	0.82	0.82
60	25.25	24.07	0.82	0.54

FT-Raman was done to study the chemical structure of prepared HAp. As shown in Figure 4 (a) and (b), the prepared HAp showed characteristic peaks at 763 and 694 cm^{-1} [24]. The band at 962 cm^{-1} was ascribed to mode υ_1 PO_4^{-3} internal modes of HAp [25-26]. The band at 1046 cm^{-1} was due to the presence of three nonequivalent PO_4^{3-} (υ_3) tetrahedral structures in β-TCP [25-26]. Additionally, it is seen that with an increase of sonication time, this is also an increase in the intensity of the broadband at around 2400-3000 cm^{-1}. These bands are also attributed to the O-H stretching mode [27]. The OH molecule was generated from the dissociation of water molecule when irradiate with ultrasonic waves [13]. Thus, preparation of HAp with the aid of ultrasonic energy might increase the quantity of OH^- in the structure of HAp [18]. Thus, a quantity of OH^- molecule affected the morphology of HAp. As highlighted by Padmanabhan *et al.* [28], the facet with high energy, i.e., the (1 1 0) plane exhibited increased OH^- concentration, and thus possibly restricted the movement of Ca^{2+} and PO_4^{3-} in the nucleus to one particular direction, i.e., [0 0 2].

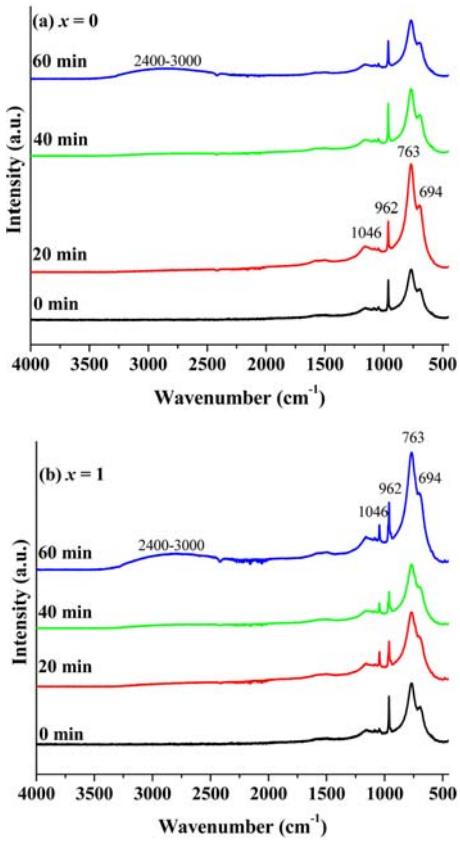

Figure 4. FT-Raman spectra of HAp (a) $x = 0$ and (b) $x = 1$.

Figure 5(a)-(d) compares the TEM images of stochiometirc HAp irradiated with ultrasonic waves for various times. Agglomerations of HAp particles were observed in all samples. It was clearly observed that ultrasonic irradiation led to the formation of very fine nano-rod HAp particles. These results agree with our previous work [17-18]. Based on the image software calculations, the diameter of prepared HAp ranged from 15 to 50 nm. The diameter tended to decrease with increasing sonication time. The might be due to the increasing of concentration of OH^- and the formation of HAp possibly occured in the interfacial region between the cavitation of bubbles and the surrounding bulk solution [29]. The effect of sonication time on non-stochiometirc HAp is presented in the TEM images of Figure 6. As expected, nano-rod HAp was obtained with increased of sonication time. Comparing Figures 5 and 6, the diameter of non-stochiometirc HAp ($x = 1$) was smaller than that of stochiometirc HAp ($x = 0$). These results also confirm that ultrasonication led to an increase in the aspect ratio of HAp particles as sonication time was increased [17,18,29]. Interestingly, a smaller diameter (*ca*- 10 nm) with much more of micro-void was observed in the case of non-stochiometirc HAp after 60 minutes of ultrasonic irradiation. Therefore, the optimum sonication time for preparation of a smaller nano rod HAp phase was 60 minutes.

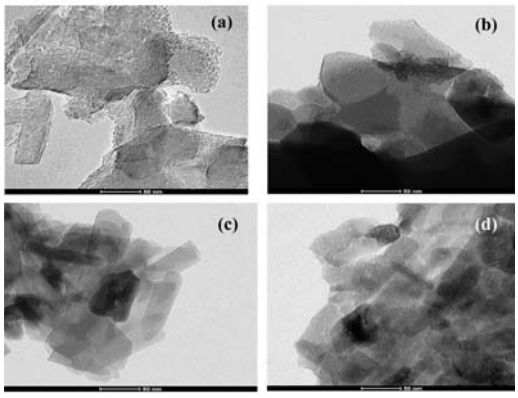

Figure 5. TEM image of synthesized HAp where $x = 0$, (a) 0 min, (b) 20 min, (c) 40 min, and (d) 60 min.

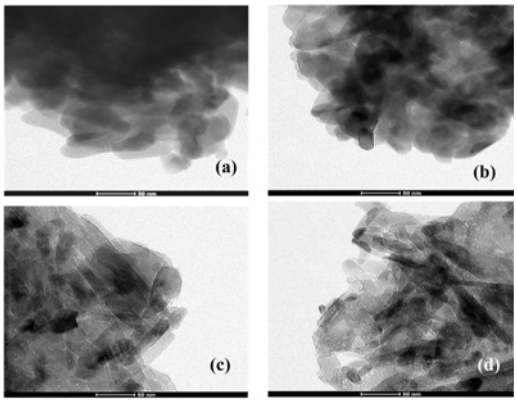

Figure 6. TEM image of synthesized HAp where $x = 1$ (a) 0 min, (b) 20 min, (c) 40 min and (d) 60 min.

4. CONCLUSIONS

In this study, nano rod HAp was successfully prepared using diluted natural rubber latex (1% DRC) as a bio-macromolecule templating agent with the aid of an ultrasonic method at 25 kHz. The natural rubber latex was completely removed with calcination at 600 °C. After that, the HAp powder was structurally analyzed. The mixed phase between HAp and β-TCP was clearly observed in all samples. The investigation also revealed that the Ca:P ratio, as well as the quantity of OH^- affected the thermal stability and morphology of the prepared HAp. The non-stochiometric HAp ($x = 1$) was more stable than the stochiometric HAp (x = 0). The quantity of OH^- increased with sonication time as confirmed by FT-Raman results. From TEM images, the morphology of all HAp sample changed from plate-like to nano rod-like particle with longer irradiation times. From

image J calculation, the diameter of non-stochiometric HAp was lower than that of stoichiometric HAp. A smaller diameter (*ca*- 10 nm) of nano rod HAp was clearly observed in case of non-stochiometric HAp after 60 minutes of sonication time.

ACKNOWLEDGEMENTS

This work was supported by Research and Development Institute (Grant No. 2557FUND08SC08-672), Udon Thani Rajabhat University, Thailand.

REFERENCES

[1] Zhou H. and Lee J., *Acta Biomater.*, 2011; **7**: 2769-2781. DOI 10.1016/j.actbio.2011.03.019.

[2] Klinkaewnarong J. and Maensiri S., *Chiang Mai J. Sci.,* 2010; **37**: 243-251.

[3] Okuda T., Loku K., Yonezawa I., Minagi H., Gonda Y., Kawachi G., Kamitakahara M., Shibata Y., Murayama H., Kurosawa H. and Ikeda T., *Biomaterials*, 2008; **29**: 2719-2728. DOI 10.1016/j.biomaterials.2008.03.028.

[4] Ng S.X., Guo J., Ma J. and Loo S.C.J., *Acta Biomater.*, 2011; **6**: 3772-3781. DOI 10.1016/j.actbio.2010.03.017.

[5] Sadat-Shojai M., Atai M., Nodehi A. and Khanlar L.N., *Dent. Mate.,* 2010; **26**: 471-482. DOI 10.1016/j.dental.2010.01.005.

[6] Uskoković V., Uskoković D.P., *J. Biomed. Mater Res. B Appl. Biomater,*. 2011; **96**: 152-91. DOI 10.1002/jbm.b.31746.

[7] Shanthi P.M, Mangalaraja R.V., Uthirakumar A.P., Velmathi S., Balasubramanian T. and Ashok M., *J. Colloid Interface Sci.*, 2010; **350**: 39-43. DOI 10.1016/j.jcis.2010.05.046.

[8] Ho C.C., Kondon T., Muramatsu N. and Ohsima H., *J. Colloid Interface Sci.*, 1996; 178: 442-445. DOI 10.1006/jcis.1996.0139.

[9] Nawamawat K., Sakdapipanich J.T., Ho C.C., Ma Y., Song J. and Vancso J.G., *Colloids Surf A.*, 2011; **390** : 157-166. DOI 10.1016/j.colsurfa.2011.09.021.

[10] Rippel M.M., Paula Leite C.A. and Galembeck F., *Anal. Chem.*, 2002; **74**: 2541-2546. DOI 10.1021/ac0111661.

[11] Nawamawat K., *Effect of Non-rubber Components on Basic Characteristics and Physical Properties of Natural Rubber from Havea Brasiliensis*, Ph.D. Thesis, Mahidol University, Thailand, 2008.

[12] Utara S. and Saengsila P., *Macromol. Symp.,* 2015; **354**: 287-293. DOI 10.1002/masy.201400050.

[13] Kharissova O.V., Kharisov B.I., Ruíz Valdés J.J. and M□éndez U.O., *Synth. React. Inorg. Me.,* 2011; **41**: 429-448. DOI 10.1080/15533174.2011.568424.

[14] Cao L.Y., Zhang C.B. and Huang J.F., *Ceram. Int.*, 2005; 31: 1041-1044. DOI 10.1016/j.ceramint.2004.11.002.

[15] Rouhani P., Taghavinia N. and Rouhani S., *Ultrason. Sonochem.,* 2010; **17**: 853-856. DOI 10.1016/j.ultsonch.2010.01.010.

[16] Gopi D., Indira J., Kavitha L., Sekar M. and Mudali U.K., *Spectro. Chim. Acta A.*, 2012; 93: 131-134. DOI 10.1016/j.saa.2012.02.033.

[17] Utara S. and Klinkaewnarong J., *Micro Nano Lett.,* 2015; **10**: 1-4. DOI 10.1049/mnl.2014.0316.

[18] Utara S. and Klinkaewnarong J., *Ceram. Int.,*2015; **10**: 14860-14867. DOI 10.1016/j.ceramint.2015.08.018.

[19] Utara S. and Boochathum P., *Polym. Plast. Technol. Eng.*, 2011; **50**: 1019-1026. DOI 10.1080/03602559.2011.557819.

[20] Klinkaewnarong J., Swatsitang E. and Maensiri S., *Solid State Sci.*, 2009;

11: 1023-1027. DOI 10.1016/j.solidstatesciences.2009.02.003.

[21] Rusu V.M., Ng C.H., Wilke M., Tiersch B., Fratzl P. and Peter M.G., *Biomaterials*, 2005; **26**: 5414-5426. DOI 10.1016/j.biomaterials.2005.01.051.

[22] Viswanath B. and Ravishanakar N., *Biomaterials*, 2008; **29**: 4855-4863. DOI 10.1016/j.biomaterials.2008.09.001.

[23] Asghar Abidi S.S. and Murtaza Q., *J. Mater. Sci. Technol.,* 2014; **30**: 307-310. DOI 10.1016/j.jmst.2013.10.011.

[24] Smith R. and Rehman I., *J. Mater. Sci. Mater. Med.*, 1995; **5**: 775-778.

[25] De Aza P., Guitian F., Santos C., De Aza S., Cusco R. and Artus L., *Chem. Mater.,* 1997; **9**: 916-922. DOI 10.1021/cm9604266.

[26] Khan A.F., Awais M., Khan A.S., Tabassum S., Chaudhry A.A. and Rehman I.U., *Appl. Spectrosc. Rev.*, 2013; **48**: 329-355. DOI 10.1080/05704928.2012.721107.

[27] Silva C.C. and Sombra A.S.B., *J. Phys. Chem. Solids,* 2004; **65**: 1031-1033. DOI 10.1016/j.jpcs.2003.10.071.

[28] Padmanabhan S.K., Balakrishnan A., Chu M.C., Lee Y.J., Kim T.N. and Cho S.J., *Particuology*, 2009; **7**: 466-470. DOI 10.1016/j.partic.2009.06.008.

[29] Jevtic M., Mitric M., Skapin S., Jancar B., Ignjatovic N., Uskokovic D., *Cryst. Growth Des.*, 2008; **8**: 2217–2222. DOI 10.1021/cg7007304.